JOURNAL OF COMPUTATIONAL PHYSICS 49, 67–93 (1983)

Computational Studies of First-Born Scattering Cross Sections II. Moment-Theory Approach

D. J. MARGOLIASH*

Department of Chemistry, Indiana University, Bloomington, Indiana 47405

AND

P. W. LANGHOFF†

Laboratoire des Collisions Atomiques et Moléculaires, Université Paris-Sud 91405 Orsay Cedex, France

Received January 21, 1982

Moment-theory methods are described for calculations of the high-energy electron impact-excitation and -ionization cross sections and closely related Van Hove correlation functions of atomic and molecular targets. The conventional Bethe–Born expressions are evaluated employing moment-theory techniques that avoid explicit construction of discrete and continuum target eigenspectra. Appropriately defined generalized-oscillator-strength spectral moments and corresponding polynomial recurrence coefficients are seen to furnish necessary and sufficient information for Born calculations. The convergence of partial-wave variational calculations of such moments and coefficients is investigated for hydrogenic targets using complete basis sets of square-integrable functions. Calculated spectral moments and recurrence coefficients, and previously devised Stieltjes–Tschebyscheff techniques, are employed in constructing Gaussian and Radau quadratures that provide convergent approximations to the corresponding Bethe surface of discrete and continuum generalized oscillator strengths, and to the associated cross sections and correlation functions. Square-integrable principal pseudostates obtained from variational calculations of multipole spectral moments are shown to provide correctly normalized convergent approximations to the discrete and continuum transition densities appropriate for the target considered, clarifying the underlying basis of reliability and numerical stability of the moment-theory approach to Bethe-Born cross sections. The development should prove particularly useful in investigations of the Bethe surfaces, related scattering cross sections, and Van Hove correlation functions of molecular targets.

I. INTRODUCTION

The Bethe–Born theory of high-energy inelastic charged-particle scattering has long provided a useful first approximation to the impact-excitation and -ionization cross

* Present address: Department of Chemistry, University of Western Ontario, London, Ontario, Canada N6A 5B7.

† Permanent address: Department of Chemistry, Indiana University, Bloomington, Indiana 47405.

0021-9991/83/010067-27$03.00/0

sections of atomic and molecular targets [1–3]. In this approach, the complete set of discrete and continuum target eigenstates are formally required, making precise evaluations of scattering cross sections cumbersome, and motivating the introduction of computationally more tractable approximations in lieu of the correct Bethe–Born results. Certain aspects of these difficulties, and of the ranges of validity of the computational approximations introduced, are described in detail in the immediately preceding publication [4]. It is indicated there that appropriately defined spectral moments provide generalized quadratures for the Bethe–Born development, suggesting an alternative approach to the evaluation of high-energy inelastic scattering cross sections that explicitly avoids construction of target eigenstates. In view of the continuing interest in studies of molecular impact-excitation and -ionization cross sections, in which cases construction of target continuum eigenfunctions is particularly troublesome, it would seem helpful to investigate further a moment-theory approach to Bethe–Born cross sections.

In the present work, Stieltjes and Tschebyscheff moment-theory approaches, previously described for constructing dipole excitation spectra in atoms and molecules [5], and in nuclei [6], are extended to the generalized oscillator-strength distributions, scattering cross sections, and related Van Hove correlation functions of electron impact-excitation spectra. As in the dipole case [7], the correct discrete and continuum eigenstates are avoided by employing basis sets of square-integrable functions in Ritz variational calculations of spectral sums, or moments, of the generalized oscillator-strength distribution. Recent extensions of the Tschebyscheff–Stieltjes–Markoff moment theory provide convergent approximations to both the discrete and continuum portions of Bethe surfaces, to corresponding scattering cross sections, and to associated Van Hove correlation functions from the calculated moments [8, 9]. In order to achieve numerical stability, recurrence coefficients for polynomials orthogonal with respect to the correct generalized oscillator-strength distribution are employed in computational applications [8–10]. Since the spectral sums and recurrence coefficients in the present case are functions of the moment transferred to the target, or of the scattering angle, detailed investigations of their convergence are in order. Atomic hydrogen provides a useful illustrative example of the computations required to determine convergent spectral moments and recurrence coefficients, and of the overall Stieltjes–Tschebyscheff approach for inelastic electron-scattering calculations. Molecular and more complex atomic targets are the subjects of subsequent theoretical investigations.

Convergent approximations to the correct Beth surface, scattering cross sections, and correlation functions in atomic hydrogen are obtained employing both conventional power moments and appropriately defined modified spectral moments [11–13]. As few as five spectral moments are found to provide results in qualitative accord with the correct Bethe surface, and convergence to the correct result is obtained upon introduction of sufficient numbers of moments or equivalent recurrence coefficients. Since the Bethe surface itself is found to be rapidly convergent in the moment-theory development, corresponding convergence of the inelastic scattering cross sections is also assured. It is emphasized that the generalized Gaussian and Radau quadratures

obained from spectral moments are optimal for the evaluation of corresponding spectral integral properties. Because the Van Hove autocorrelation functions for target atom electrons are found to be particularly sensitive to the moment-theory procedures, detailed evaluations of these are also reported. Finally, square-integrable principal pseudostates obtained from Hilbert-space variational calculations and the Stieltjes–Tschebyscheff development are shown to provide convergent approximations to the appropriate discrete and continuum transition densities, and to clarify the underlying basis of reliability and numerical stability of the L^2 moment approach [14–16]. The Stieltjes and Tschebyscheff methods are consequently seen to furnish all the scattering and excitation information customarily obtained from explicit construction of discrete and continuum target eigenstates, and, consequently, should prove particularly useful in subsequent investigations of the Bethe surfaces, related scattering cross sections, and Van Hove correlation function of complex atoms and molecules.

In Section II, the invariant momentum-transfer (or scattering angle dependent) spectral moments are defined and techniques for their evaluation are described. Aspects of the Tschebyscheff–Stieltjes–Markoff moment theory and the Stieltjes and Tschebyscheff derivatives are described briefly in Section III, and detailed computational results are presented and discussed in Section IV. Some general and concluding remarks are made in Section V.

II. Spectral Moments

The invariant spectral moments of the generalized oscillator-strength distribution of an atomic or molecular target are conveniently written in the form [12, 13]

$$S(q, i) = \int_{\varepsilon_1}^{\infty} \varepsilon^i \, df(\varepsilon, q). \tag{1}$$

Here, ε_1 is the first transition energy, the index i is restricted to integer values for which convergence is assured, and $df(\varepsilon, q)$ is the generalized oscillator strength for target transition into the excitation energy interval ε to $\varepsilon + d\varepsilon$ upon transfer of momentum q from the scattering projectile [4]. The generalized oscillator-strength distribution can be written in the form

$$f(\varepsilon, q) = \int_{\varepsilon_1}^{\varepsilon} df(\varepsilon', q) = \int_{\varepsilon_1}^{\varepsilon} \left[\sum_{n=1}^{\infty} f_n(q) \, \delta(\varepsilon_n - \varepsilon') + g(\varepsilon', q) \right] d\varepsilon', \tag{2}$$

where $f_n(q)$ and $g(\varepsilon, q)$ are the discrete and continuum strengths, respectively, and ε_n are the corresponding discrete excitation energies. The term in square brackets in Eq. (2) defines the generalized oscillator-strength density, which is seen to include delta-function contributions from discrete transitions and a smooth portion associated with the impact-ionization continuum. Since $df(\varepsilon, q) \geqslant 0$ for ground state targets,

$f(\varepsilon, q)$ is a nondecreasing function of ε for fixed q or scattering angle θ. Such distributions are characterized uniquely by their power moments. A sufficient number of moments, or closely related polynomial recurrence coefficients described below [8], provides the necessary and sufficient information for construction of accurate approximations to the distribution $f(\varepsilon, q)$ and to the corresponding density [5–16].

To demonstrate that the moments of Eq. (1) can be computed without reference to the eigenstates required in construction of $f_n(q)$ and $g(\varepsilon, q)$, note that enforcing closure in the usual way gives [4]

$$S(q, i) = 2\langle\phi_0|\,(1/q)\exp(-i\mathbf{q}\cdot\mathbf{r})(H_0 - E_0)^{i+1}(1/q)\exp(i\mathbf{q}\cdot\mathbf{r}\,|\,\phi_0\rangle. \tag{3}$$

Here, H_0, E_0, and ϕ_0 are the target Hamiltonian, ground-state energy, and wave function, respectively, $(H_0 - E_0)^{i+1}$ is defined in the subspace orthogonal to ϕ_0, and a one-electron target is considered for notational convenience. In the cases $i = 2, 1, 0,$ and -1, Eq. (3) provides sum rules in the form of expectation values over ϕ_0 [17]. In the cases $i = -k$, $k \geqslant 2$, the sums of Eq. (3) can be written in the forms [11 – 13]

$$S(q, -k) = 2\langle\theta_k|\,(1/q)\exp(i\mathbf{q}\cdot\mathbf{r})\,|\,\phi_0\rangle, \tag{4}$$

where the so-called Cauchy functions θ_k are given by [11–13]

$$\theta_k \equiv (H_0 - E_0)^{1-k}(1/q)\exp(i\mathbf{q}\cdot\mathbf{r})\,\phi_0, \qquad k = 2, 3, 4,..., \tag{5}$$

with $(H_0 - E_0)^{1-k}$ defined in the subspace of the target Hamiltonian H_0 orthogonal to ϕ_0, as in Eq. (3). From Eqs. (3) and (5),

$$\langle\theta_k\,|\,\theta_l\rangle = (1/2)\,S(q, 1 - k - l), \tag{6}$$

indicating that the θ_k are square-integrable functions for all q when the moments $S(q, 1 - 2k)$ are finite, suggesting that they can be computed in a complete L^2 basis set without explicit reference to the target spectral functions.

The θ_k of Eq. (5) are conveniently obtained from the equations [18]

$$(H_0 - E_0)\,\theta_2 = (1/q)\exp(i\mathbf{q}\cdot\mathbf{r})\,\phi_0, \tag{7a}$$

$$(H_0 - E_0)\,\theta_k = \theta_{k-1}, \qquad k \geqslant 3, \tag{7b}$$

where the particular solutions required are those orthogonal to ϕ_0. Although the functions θ_k can perhaps be obtained in closed form for simple model systems, a more general strategy is required for complex atoms and molecules. In the case of atomic systems, a conventional partial-wave expansion is conveniently employed [12, 13].

Introduction of a partial-wave expansion in the development of Eqs. (1)–(7) gives corresponding expressions for the spectral moments

$$S(q, i) = \sum_{l=0}^{\infty} S^{(l)}(q, i), \tag{8a}$$

generalized oscillator-strength distribution

$$f(\varepsilon, q) = \sum_{l=0}^{\infty} f^{(l)}(\varepsilon, q), \tag{8b}$$

and Cauchy functions

$$\theta_k = \sum_{l=0}^{\infty} \theta_k^{(l)}. \tag{8c}$$

These partial-wave Cauchy functions $\theta_k^{(l)}$ and moments $S^{(l)}(q, i)$ can be constructed employing conventional computational methods [18, 19]. It is convenient to perform the necessary variational calculations using square-integrable pseudostates that satisfy

$$\langle \tilde{\phi}_i^{(l)} | H_0 - E_0 | \tilde{\phi}_j^{(l)} \rangle = \delta_{ij} \tilde{\varepsilon}_i^{(l)}, \tag{9a}$$

$$\langle \tilde{\phi}_i^{(l)} | \tilde{\phi}_j^{(l)} \rangle = \delta_{ij}, \qquad i, j = 1, 2, \ldots, N, \tag{9b}$$

for the lth partial wave. Approximations to the Cauchy functions $\theta_k^{(l)}$ and spectral sums $S^{(l)}(q, i)$ are obtained from the functions of Eqs. (9) in the forms

$$\tilde{\theta}_k^{(l)} = \sum_{j=1}^{N} \tilde{\phi}_j^{(l)} [\tilde{\varepsilon}_j^{(l)}]^{1-k} \langle \tilde{\phi}_j^{(l)} | (1/q) \exp(i\mathbf{q} \cdot \mathbf{r}) | \phi_0 \rangle \tag{10a}$$

$$\tilde{S}^{(l)}(q, i) = \sum_{j=1}^{N} [\tilde{\varepsilon}_j^{(l)}]^i \tilde{f}_j^{(l)}(q), \tag{10b}$$

where

$$\tilde{f}_j^{(l)}(q) = 2\tilde{\varepsilon}_j^{(l)} |\langle \tilde{\phi}_j^{(l)} | (1/q) \exp(i\mathbf{q} \cdot \mathbf{r}) | \phi_0 \rangle|^2 \tag{11}$$

is the pseudostrength associated with the pseudotransition frequency $\tilde{\varepsilon}_j^{(l)}$. In view of Eq. (6), $\tilde{S}^{(l)}(q, i)$ will converge to $S^{(l)}(q, i)$ in the limit $N \to \infty$, provided the L^2 basis employed in calculating the $\tilde{\phi}_i^{(l)}$ of Eqs. (9) spans both discrete and continuum portions of the l-wave spectrum of H_0. Convergence of the partial-wave expansion of Eqs. (8) will usually be limited to sufficiently small values of q, since a finite number of waves must generally be employed. It is important to recognize in this connection, however, that the large-q limits of the moments, distributions, and Cauchy functions of Eqs. (8) are controlled in large measure by the binary-encounter approximation [4], since the corresponding Bethe surface is dominated by the Bethe ridge for the atom or molecule studied [1–3]. Consequently, the variational development of Eqs. (8)–(11) should be regarded as appropriate for those portions of the Bethe surface in which the distinctive atomic or molecular nature of the excitation spectrum dominates, generally corresponding to small and intermediate q and ε values [1 – 3].

It is useful to also consider so-called modified moments of the generalized oscillator-strength distribution, defined according to [20]

$$M(q, i) = \int_{\varepsilon_1}^{\infty} p_i(\varepsilon)\, df(\varepsilon, q), \tag{12}$$

where the $p_i(\varepsilon)$ are polynomials in the variable ε orthogonal with respect to an appropriate reference density [10]. Since the polynomials $p_i(\varepsilon)$ can be chosen to evenly weight the entire spectrum for all i, the moments of Eq. (12) provide a useful alternative to the power moments of Eq. (1), which predominantly weight the low-frequency region of the spectrum as $i \to -\infty$. Consequently, for spectral moments of a specified accuracy, the moment problem resulting from the use of polynomial moments is generally more stable than that resulting from power moments [21]. In order to utilize this greater stability however, it is generally necessary that the moments of Eq. (12) be computed without recourse to the power moments of Eq. (1), since construction of the former directly from the latter can lead to a compensating loss of accuracy [22].

III. Stieltjes–Tschebyscheff Moment-Theory Techniques

When sufficiently accurate approximations to spectral sums (Eq. (1)) or related polynomial moments (Eq. (12)) are available, previously described Stieltjes and Tschebyscheff techniques [5–9] can be employed to construct the appropriate Bethe surface, associated cross sections, and Van Hove correlation functions [4]. These procedures entail determinations of generalized Gaussian and Radau quadratures from the given moments [8], which quadratures are then employed in construction of Stieltjes and Tschebyscheff approximations, respectively, to the corresponding distribution and density. Since the development has been described in considerable detail previously, only those aspects of the theory specifically required for clarity are presented here.

The nth-order generalized Gaussian quadratures $(\varepsilon_i(q, n), f_i(q, n); i = 1, n)$ required in the Stieltjes development satisfy the equations [8, 9]

$$S(q, -k) = \sum_{i=1}^{n} \varepsilon_i(q, n)^{-k} f_i(q, n), \qquad k = 0, 1, \ldots, 2n-1, \tag{13}$$

where the $S(q, -k)$ are the defining moments of Eq. (1). Equations (13) are written arbitrarily for the indicated range $(k = 0, \ldots, 2n-1)$ of spectral moments, although any $2n$ sequential values can be employed in the development. Note in this connection that the θ_k of Eqs. (4)–(7) are well defined for any k giving a convergent moment. Explicit expressions for the Stieltjes approximations to the distribution and

density are obtained from the quadratures of Eq. (13) in the histogram forms [14–16]

$$f^{(n)}(\varepsilon, q) = \sum_{i=1}^{j} f_i(q, n), \qquad \varepsilon_j(q, n) < \varepsilon < \varepsilon_{j+1}(q, n) \tag{14a}$$

$$g^{(n)}(\varepsilon, q) = \tfrac{1}{2}[f_{j+1}(q, n) + f_j(q, n)]/[\varepsilon_{j+1}(q, n) - \varepsilon_j(q, n)], \qquad \varepsilon_j(q, n) < \varepsilon < \varepsilon_{j+1}(q, n). \tag{14b}$$

The histogram of Eq. (14b) corresponds to a finite-difference approximation to the correct density constructed from the distribution histogram of Eq. (14a) [14–16]. Both distribution and density histograms converge to the correct corresponding results in the limit $n \to \infty$ [9].

The nth-order Radau quadratures $[\varepsilon_i(q, \varepsilon, n), f_i(q, \varepsilon, n); i = 0, n]$ of interest here are given by the equations [8, 9]

$$S(q, -k) = \varepsilon^{-k} f_0(q, \varepsilon, n) + \sum_{i=1}^{n} \varepsilon_i(q, \varepsilon, n)^{-k} f_i(q, \varepsilon, n), \qquad k = 0,..., 2n, \tag{15}$$

where $f_0(q, \varepsilon, n)$, the n values of $\varepsilon_i(q, \varepsilon, n)$, and the n values of $f_i(q, \varepsilon, n)$ are functions of a prespecified point ε ($\equiv \varepsilon_0(q, \varepsilon, n)$), as indicated. Since ε can be prespecified, the quadratures of Eq. (15) provide an approximation to the distribution at any point in the spectrum in the form [23–25]

$$F^{(n)}(\varepsilon, q) = \sum_{i=1}^{m} f_i(q, \varepsilon, n) + \tfrac{1}{2} f_0(q, \varepsilon, n), \tag{16a}$$

where the sum in i is over the m values of $f_i(q, \varepsilon, n)$ associated with points $\varepsilon_i(q, \varepsilon, n) < \varepsilon$. A corresponding approximation to the density $g(\varepsilon, q)$ is obtained from the derivative of Eq. (16a) in the form [9]

$$G^{(n)}(\varepsilon, q) \equiv \frac{dF^{(n)}(\varepsilon, q)}{d\varepsilon} = \sum_{i=1}^{m} \frac{df_i(q, \varepsilon, n)}{d\varepsilon} + \frac{1}{2} \frac{df_0(q, \varepsilon, n)}{d\varepsilon}. \tag{16b}$$

Equation (16b) provides a Tschebyscheff approximation to $g(\varepsilon, q)$ which is generally smooth in the continuum portion of the spectrum but gives delta-function-like behavior at the appropriate discrete transition frequencies [9, 23–25]. When the prespecified value ε is set at a generalized Gaussian quadrature point of order $n + 1$ (Eq. (13)), the density of Eq. (16b) is closely related to the Stieltjes derivative of order $n + 1$, which latter is obtained from the conventional finite-difference approximation of Eqs. (14) [9]. The Tschebyscheff aproximations to the distribution and density converge to the appropriate correct values in the limit of large n [9].

The Tschebyscheff density of Eq. (16b) is a rational function of ε and the $\varepsilon_i(q, \varepsilon, n)$ which is nonnegative on the real axis with $2n - 2$ continuous derivatives, and has poles in the upper and lower complex plane [9]. The locations of these poles are distinct from the $\varepsilon_i(q, \varepsilon, n)$, which latter are real and are the roots of quasi-orthogonal

polynomials having a fixed real root ε [8]. The complex poles generally have very small imaginary parts when their real parts are in the discrete portion of the spectrum, and they apparently converge to the correct discrete frequencies on the real axis in the limit of large n [23].

Although the foregoing development focuses attention on the extraction of spectral information from calculated moments (Eqs. (1)–(12)), prodecures for solution of Eqs. (13) and (15) generally avoid manipulations involving the spectral moments. Rather, so-called recurrence coefficients for the polynomials orthogonal with respect to the correct generalized oscillator-strength density are generally preferred in computational applications [5, 6]. The appropriate recurrence relations are [24]

$$P_n(\varepsilon, q) = (1 - \alpha_n(q)\,\varepsilon)\,P_{n-1}(\varepsilon, q) - \varepsilon^2 \beta_{n-1}(q)\,P_{n-2}(\varepsilon, q) \tag{17a}$$

$$P_0(\varepsilon, q) = 1, \qquad P_{-1}(\varepsilon, q) = 0, \tag{17b}$$

where $\alpha_n(q)$, $\beta_n(q)$ are the recurrence coefficients, and the polynomials $P_n(\varepsilon, q)$ satisfy the orghogonality conditions

$$\int_{\varepsilon_1}^{\infty} (1/\varepsilon)^{n+m}\,P_n(\varepsilon, q)\,P_m(\varepsilon, q)\,df(\varepsilon, q) = N_n(q)\,\delta_{nm}, \tag{18a}$$

with

$$N_n(q) = \beta_0(q)\,\beta_1(q) \cdots \beta_n(q). \tag{18b}$$

The coefficients $\alpha_n(q)$, $\beta_n(q)$ are obtained from a computationally stable procedure employing the expressions [24]

$$\alpha_n(q) = \frac{1}{\beta_0(q) \cdots \beta_{n-1}(q)} \int_{\varepsilon_1}^{\infty} (1/\varepsilon)^{2n-1}\,P_{n-1}(\varepsilon, q)^2\,df(\varepsilon, q) \tag{19a}$$

$$\beta_n(q) = \frac{1}{\beta_0(q) \cdots \beta_{n-1}(q)} \int_{\varepsilon_1}^{\infty} (1/\varepsilon)^{2n}\,P_n(\varepsilon, q)^2\,df(\varepsilon, q). \tag{19b}$$

When a pseudo-spectral representation of $f(\varepsilon, q)$ calculated in an L^2 basis (Eqs. (8)–(11)) is used, the recurrence relation of Eqs. (17) is conveniently employed to generate the necessary polynomial values appearing in Eqs. (19) at the pseudo eigenvalues with considerable numerical stability. All required quantities are then obtained from the calculated recurrence coefficients following procedures described previously in considerable detail [9, 24]. The major computational step involved entails diagonalization of the symmetric tridiagonal matrix

$$\mathbf{M}^{(n)}(q) = \begin{bmatrix} \alpha_1(q) & \beta_1(q)^{1/2} & 0 & 0 & \cdots & 0 \\ \beta_1(q)^{1/2} & \alpha_2(q) & \beta_2(q)^{1/2} & 0 & \cdots & 0 \\ 0 & \beta_2(q)^{1/2} & \alpha_3(q) & \beta_3(q)^{1/2} & \cdots & 0 \\ \vdots & \vdots & \vdots & \vdots & \ddots & \vdots \\ 0 & 0 & 0 & 0 & \cdots & \alpha_n(q) \end{bmatrix} \tag{20}$$

from which the Gaussian quadratures $\varepsilon_i(q, n)$, $f_i(q, n)$ of Eq. (13) are obtained. The Radau quadrature points and weights of Eq. (15) are obtained from diagonalization of a closely related matrix, with $\alpha_n(q)$ in Eq. (20) replaced by $\varepsilon - \beta_{n-1}(q)\, P_{n-2}(\varepsilon)/P_{n-1}(\varepsilon)$.

IV. Application to Hydrogenic Targets

Atomic hydrogen provides a useful example for investigating convergence of the moment-theory approach to Bethe surfaces, scattering cross sections, and correlation functions, and for illustrating and verifying the development described in the foregoing sections. The discrete and continuum portions of the generalized oscillator-strength spectra and corresponding moments, cross sections, and correlation functions are given explicitly in the preceding publication [4]. Introduction of the familiar Rayleigh expansion of a plane wave into the oscillator strengths and density gives the partial-wave contributions to the discrete and continuum portions of the Bethe surface in atomic hydrogen. Since these expressions are somewhat lengthy, they are not reproduced here. Their $q \to 0$ limits, however, are proportional to the so-called multipole oscillator-strength distributions in atomic hydrogen, which can be written in the compact forms [26]

$$\varepsilon_n^{(l)} = \tfrac{1}{2}[1 - (1/n)^2], \qquad n = 2, 3,..., \tag{21a}$$

$$f_n^{(l)} = \frac{8l^2}{(2l+1)} \frac{(n+l)!}{(n-l-1)!} \frac{\varepsilon_n}{(n\varepsilon_n)^{(2l+4)}} \left(\frac{n-1}{n+1}\right)^{2n}, \qquad n = 2, 3,..., \tag{21b}$$

$$g^{(l)}(\varepsilon) = \frac{8l^2}{2l+1} \frac{1}{\varepsilon^{(2l+3)}} \left[\prod_{j=1}^{l} (1 + j^2 k(\varepsilon)^2)\right] \times \frac{\exp[-(4/k(\varepsilon)) \tan^{-1}(k(\varepsilon))]}{1 - \exp[-2\pi/k(\varepsilon)]}, \tag{21c}$$

$$k(\varepsilon) = (2\varepsilon - 1)^{1/2}, \qquad \tfrac{1}{2} \leqslant \varepsilon < \infty. \tag{21d}$$

Equations (21) provide information useful for investigation of the principal pseudostate representations of l-wave Coulomb continuum functions in atomic hydrogen described in subsection *D* below.

A. *Spectral Moments and Polynomial Recurrence Coefficients*

Basic sets of associated Laguerre functions of order $n + l + 1/2l + 2$ are employed in variational calculations (Eqs. (8)–(11)) of the spectral sums for atomic hydrogen [27]. These functions are chosen because they are L^2 complete in R^1 for all l. Moreover, a finite number of them for given l span the space of an equal number of corresponding multipole Cauchy functions in atomic hydrogen [28]. Consequently, a variational calculation employing N such functions reproduces the first $2N$ of the multipole moments of the spectrum of Eqs. (21).

TABLE I

Variationally Determined Values of the Bethe Sum Rule $S(q, 0) = 1$ in Atomic Hydrogen[a]

$L\backslash N$[b]	10	20	30	40	50
			$q = 1$		
4	0.99418	0.99417	0.99417	0.99417	0.99417
9	1.00001	1.00000	1.00000	1.00000	1.00000
14	1.00001	1.00000	1.00000	1.00000	1.00000
19	1.00001	1.00000	1.00000	1.00000	1.00000
24	1.00001	1.00000	1.00000	1.00000	1.00000
			$q = 2$		
4	0.90531	0.90513	0.90513	0.90513	0.90513
9	0.99816	0.99809	0.99809	0.99809	0.99809
14	1.00004	0.99997	0.99997	0.99997	0.99997
19	1.00006	1.00000	1.00000	1.00000	.00000
24	1.00006	1.00000	1.00000	1.00000	1.00000
			$q = 3$		
4	0.74758	0.74761	0.74732	0.74730	0.74730
9	0.93124	0.97813	0.97804	0.97801	0.97801
14	0.93605	0.99855	0.99860	0.99858	0.99858
19	0.93609	0.99982	0.99994	0.99992	0.99992
24	0.93609	0.99986	1.00002	1.000000	1.000000
			$q = 4$		
4	0.48275	0.59261	0.59664	0.59640	0.59639
9	0.53946	0.91240	0.92607	0.92662	0.92664
14	0.53984	0.95253	0.98817	0.98965	0.98973
19	0.53984	0.95357	0.99643	0.99861	0.99873
24	0.53984	0.95358	0.99691	0.99971	0.99985
			$q = 5$		
4	0.19825	0.45446	0.47240	0.47473	0.47517
9	0.20539	0.71723	0.83760	0.85045	0.85243
14	0.20540	0.72707	0.92924	0.96181	0.96637
19	0.20540	0.72712	0.93414	0.98466	0.99211
24	0.20540	0.72712	0.93419	0.98627	0.99695

[a] Values, in Hartree atomic units, obtained from the development of Eqs. (8)–(11) employing Laguerre basis functions of order $n + l + 1/2l + 2$ [27 and 28].

[b] Numbers of partial waves (L) and basis functions (N) employed in the variational calculations of Eqs. (8)–(11).

Conventional procedures are used in accomplishing the diagonalizations of Eqs. (9), and the generalized oscillator strengths of Eq. (11) are evaluated employing refinements of previously described integral expressions [28, 29]. The resulting individual partial-wave contributions (Eq. (10b)) to the sum of Eq. (8a) are found to converge in the expected fashion, with the moment $S^{(l)}(1-2k)$ requiring at least k functions. In order to achieve convergence of the total q-dependent spectral moments, sufficient numbers (L) of partial waves must be included in the sum of Eq. (8a). These points are illustrated in Table I, where values of the Bethe sum rule $S(q, 0) = 1$ are shown as functions of L and N (Eqs. (8a) and 10b)). It is seen that convergence for the smaller q values is generally more rapid in L than for larger q values. This is in accord with the shapes of the corresponding portions of the Bethe surface, which extend to higher energy with increasing momentum transfer, consequently requiring more partial waves in order to achieve spectral completeness for higher q values.

Comparison of the lowest-energy pseudo-oscillator strengths (Eq. (11)) obtained from the variational calculations with the corresponding correct values indicates that convergence has been achieved in these cases. The higher-energy pseudo-oscillator strengths, of course, generally do not correspond to the correct discrete values but rather are associated with energies that fall in the continuum. The specific forms of the discrete and continuum pseudostates in atomic hydrogen obtained from the present calculations are discussed explicitly further below [Section IV(D)].

Partial-wave summations for the first five moments $S(q, k)$, $-2 \leqslant k \leqslant 2$, are shown in Fig. 1, where it is seen that the higher angular momentum values contribute significantly to the Bethe sum rule for $q > 1$. In order to obtain a convergent Bethe sum $S(q, 0)$ in this case for $0 \leqslant q \leqslant 5$ a.u., more than ten partial waves are evidently required. The $S(q, 2)$ and $S(q, 1)$ sums are found to be more slowly convergent with L, whereas the negative moments are more rapidly convergent than is the Bethe sum rule in the interval $0 \leqslant q \leqslant 5$ a.u. Consequently, convergent values for the moments

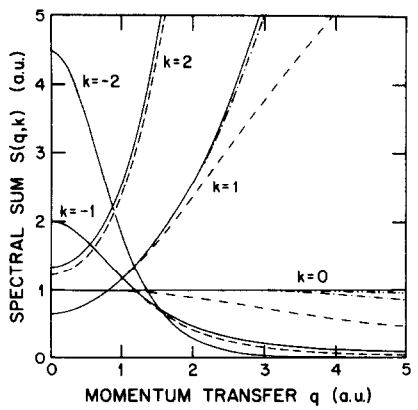

FIG. 1. Spectral sums $S(q, k)$ $(2 \geqslant k \geqslant -2)$ for the Bethe surface in atomic hydrogen: (—) exact values [4]; partial-wave summations obtained from 50-term pseudostate calculations: (---) $l = 0$–4, (–·–·–) $l = 0$–9, (–···–) $l = 0$–14. All values in Hartree atomic units.

TABLE II

Variationally Determined Polynomial Recurrence Coefficients for the Bethe Surface in Atomic Hydrogen[a]

k	$\alpha_k(q=0)$	$\alpha_k(q=1)$	$\alpha_k(q=2)$	$\alpha_k(q=3)$	$\alpha(q=4)$	$\alpha_k(q=5)$
1	2.00000	1.18080	0.46875	0.22023	0.12479	0.07992
2	1.50000	1.71328	1.33350	0.84909	0.52214	0.32204
3	1.33333	1.49257	1.65432	1.76916	1.86021	1.92494
4	1.25000	1.32667	1.39877	1.41963	1.42548	1.42751
5	1.20000	1.24430	1.29169	1.30359	1.30070	1.29354
6	1.16667	1.19534	1.22810	1.23971	1.23850	1.23174
7	1.14286	1.16294	1.18590	1.19679	1.19782	1.19253
8	1.12500	1.13985	1.15643	1.16568	1.16796	1.16314
9	1.11111	1.12254	1.13498	1.14233	1.14491	1.13943
10	1.10000	1.10907	1.11875	1.12442	1.12664	1.11975
11	1.09091	1.09828	1.10603	1.11041	1.11196	1.10357
12	1.08333	1.08944	1.09579	1.09925	1.10003	1.09092
13	1.07692	1.08206	1.08736	1.09016	1.09023	1.08174
14	1.07143	1.07581	1.08030	1.08261	1.08200	1.07544
15	1.06667	1.07045	1.07431	1.07623	1.07492	1.07093
16	1.06238	1.06580	1.06914	1.07077	1.06875	1.06707
17	1.04671	1.06245	1.06454	1.06598	1.06346	1.06324

k	$\beta_k(q=0)$	$\beta_k(q=1)$	$\beta_k(q=2)$	$\beta_k(q=3)$	$\beta_k(q=4)$	$\beta_k(q=5)$
0	1.00000	1.000000	1.000000	0.999996	0.999852	0.996946
1	0.500000	0.380404	0.072768	0.010486	0.001921	0.000479
2	0.416667	0.530903	0.632651	0.557283	0.410724	0.275934
3	0.375000	0.417494	0.471342	0.500827	0.508921	0.509931
4	0.350000	0.372728	0.395660	0.414703	0.428004	0.437081
5	0.333333	0.347886	0.359439	0.368472	0.377192	0.385353
6	0.321429	0.331569	0.338997	0.342758	0.347499	0.353626
7	0.312500	0.319964	0.325565	0.327049	0.329345	0.334036
8	0.305556	0.311279	0.315777	0.316481	0.317496	0.321714
9	0.300000	0.304528	0.308222	0.308751	0.309247	0.313775
10	0.295455	0.299127	0.302204	0.302727	0.303150	0.308347
11	0.291667	0.294706	0.297302	0.297829	0.298389	0.304094
12	0.288462	0.291018	0.293236	0.293746	0.294508	0.300119
13	0.285714	0.287895	0.289810	0.290292	0.291270	0.296035
14	0.283333	0.285215	0.286884	0.287335	0.288559	0.291958
15	0.281249	0.282891	0.284358	0.284778	0.286290	0.288255
16	0.280192	0.280828	0.282162	0.282549	0.284336	0.285210

[a] Values, in Hartree atomic units, obtained from the development of Eqs. (17)–(19) and variationally calculated pseudospectra of Eqs. (8)–(11) employing 50 basis functions and 25 partial waves in each case. The correct asymptotic ($k \to \infty$) values (Eqs. (22)) in this case are $\alpha_\infty = 1$, $\beta_\infty = 1/4$ for all q.

$S(k)$, $k = 0, -1, \ldots$, are obtained in the interval $0 \leqslant q \leqslant 5$ a.u. employing 25 partial waves in each case. Moreover, since the higher-order negative-integer moments satisfy the asymptotic behaviors $S(q \to \infty, -k) \to (2/q^2)^k$ [30], which behavior is largely a consequence of the validity of the binary-encounter approximation at large q and ε, [2] they do not have to be determined explicitly by computation for all values of momentum transfer. Rather, the partial-wave variational calculations are required only to determine the moments and corresponding recurrence coefficients for small and intermediate q values.

The variationally determined pseudospectra obtained from Eqs. (9) and (11) for $N = 50$ and $L = 24$ are employed in conjunction with Eqs. (17)–(19) to determine the corresponding polynomial recurrence coefficients shown in Table II. Comparisons of these variationally determined coefficients with the corresponding correct values (not shown) [28] indicates convergence to many significant figures has been achieved in all cases but $q = 4$ and 5 a.u., for which two or three significant figures are obtained. Moreover the calculated coefficients are seen to approach the correct asymptotic values [24]

$$\alpha_{n\to\infty}(q) \to \alpha_\infty = 1/(2\varepsilon_\infty) \tag{22a}$$

$$\beta_{n\to\infty}(q) \to \beta_\infty = 1/(4\varepsilon_\infty)^2, \tag{22b}$$

smoothly from above in every case. These values are employed in the Stieltjes–Tschebyscheff development of Section III in constructing convergent approximations to the corresponding generalized oscillator-strength distribution.

B. *Bethe Surface*

In Figs. 2 and 3, we show continuum portions $g(\varepsilon, q)$ of the Bethe surface in atomic hydrogen for five values of momentum transfer [4]. A logarithmic abscissa is employed, since the large-q profiles are flat and broad, extending to very high excitation energy, although each curve is unity normalized ($S(q, 0) = 1$). In contrast to the profiles shown in Figs. 2 and 3, which, as functions of logarithmic excitation energy, broaden with increasing fixed momentum transfer, constant-energy profiles on the Bethe surface regarded as functions of $\ln(q^2)$ becomes sharper with increasing excitation energy [2]. These features are characteristic of the so-called Bethe ridge, which dominates the high ε and q portion of the Bethe surface.

In Fig. 2a, we show Stieltjes histogram approximations (Eqs. (13) and (14)) to the five spectra in atomic hydrogen for the indicated q values, constructed using 20 negative-integer spectral moments beginning with $k = 0$, corresponding to the use of 10 $\alpha_k(q)$ and 10 $\beta_k(q)$ values (Table II), in each case. Although the Stieltjes histograms of Fig. 2a are relatively coarse, they are in general agreement with the correct profiles for the low-q curves. The Stieltjes approximations to the high-q profiles are perhaps less satisfactory, suggesting, as might be expected, that extended distributions are not as well characterized by a moderate number of their negative-integer power moments as are more compact distributions.

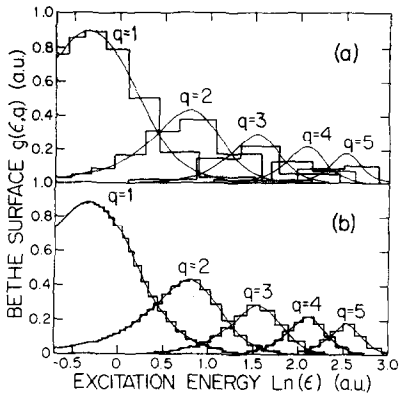

FIG. 2. Bethe surface in atomic hydrogen; light line (—) exact values of $g(\varepsilon, q)$ in each case [4]; (a) (—) tenth-order Stieltjes histograms (Eqs. (13) and (14) for $n = 10$) obtained by employing 20 calculated polynomial recurrence coefficients [Table II]; (b) (—) Stieltjes histograms (Eqs. (13) and (14)) obtained by employing 34 calculated recurrence coefficients (Table II) and the extension procedure of Eqs. (22) and (23), as discussed in the text. All values in Hartree atomic units.

As additional numbers of moments are employed in the Stieltjes development (Eqs. (13) and (14)), histograms are generated that are in increasingly good agreement with the correct density. Since the variationally determined spectral moments and associated polynomial recurrence coefficients rapidly approach known asymptotic values (Eqs. (22)) with increasing order, as is indicated explicitly in

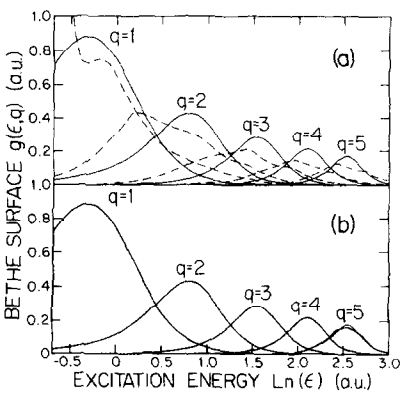

FIG. 3. Bethe surface in atomic hydrogen; light line (—) exact values of $g(\varepsilon, q)$ in each case [4]; (a) (---) second-order Tschebycheff derivative obtained from Eqs. (15) and (16) for $n = 2$; (b) (—) convergent Tschebyscheff derivatives ($q = 1$ to 4 a.u.) obtained from Eqs. (15) and (16) employing 34 calculated recurrence coefficients [Table II] and the extension procedure of Eqs. (22) and (23), as discussed in the text. All values in Hartree atomic units.

Table II, it is convenient to supplement the accurately calculated values with additional coefficients of the forms

$$\alpha_n(q) = \alpha_\infty(1 + \delta_1(q)/n + \delta_2(q)/n^2 + \cdots), \tag{23a}$$

$$\beta_{n-1}(q) = \beta_\infty(1 + \gamma_1(q)/n + \gamma_2(q)/n^2 + \cdots), \qquad n = 1, 2,.... \tag{23b}$$

Here, α_∞, β_∞ are the correct asymptotic values of the recurrence coefficients in atomic hydrogen (Eqs. (22)), and the parameters $\delta_i(q)$ and $\gamma_i(q)$ are chosen (Table III) to reproduce the highest-order accurately calculated recurrence coefficients. The specific forms of Eqs. (23) correspond to asymptotic expansions for large n and are appropriate for all q values, and for all atomic and molecular systems.

In Fig. 2b are shown Stieltjes histograms of various orders obtained by employing 34 accurate spectral moments and sufficient numbers of additional asymptotic coefficients (Eqs. (22) and (23)) to obtain smooth results. For the lower-q profiles, ~50th-order histograms are employed, whereas Stieltjes histograms of ~90th order are used for the higher-q profiles. Evidently, the Stieltjes histograms so obtained are in good agreement with the correct values in every case, and the $q = 1$ and 2 results are essentially fully converged to smooth curves for low excitation energies. These results indicate that modest numbers of accurate power moments obtained from L^2 variational calculations provide fully convergent Stieltjes densities when the appropriate asymptotic behaviors (Eqs. (22) and (23)) of the polynomial recurrence coefficients are incorporated. It should be noted that this observation is not necessarily limited to hydrogenic targets, since Eqs. (22) and (23) are valid for systems of arbitrary complexity. Use of the asymptotically correct recurrence coefficients corresponds equivalently to introduction of information corresponding to large number of highly accurate spectral moments, which cannot be employed explicitly in Eq. (13) because of numerical instabilities [21, 24, 31].

TABLE III

Extension Parameters for Asymptotic Polynomial Recurrence Coefficients in Atomic Hydrogen[a]

q	$\delta_1(q)$	$\delta_2(q)$	$\gamma_1(q)$	$\gamma_2(q)$
0	0.99750	0.02752	1.9999	0.00127
1	0.98871	1.0195	1.9758	2.0533
2	0.96776	2.1970	1.9814	3.4731
3	0.94168	3.0186	2.0148	3.3751
4	0.83840	4.2865	2.1925	1.7772
5	0.81586	3.6294	2.3703	2.2526

[a] Values, in Hartree atomic units, of the parameters appearing in the asymptotic polynomial recurrence coefficients of Eqs. (23) for the Bethe surface in atomic hydrogen.

The five spectral sums shown in Fig. 1 are employed in the development of Eqs. (15) and (16) to obtain a low-order ($n = 2$) Tschebyscheff-derivative approximation to the Bethe surface in atomic hydrogen. The continuum portions of the spectra so obtained are shown in Fig. 3a. Evidently, the very low order Tschebyscheff results of Eq. (16b) obtained by employing only five spectral moments are in qualitative accord with the correct spectra indicated in the figure. These results are of considerable interest in that four of the five sums employed are sum rules (Eq. (3)), obtained from the ground-state eigenfunction alone [17].

As in the Stieltjes development of Fig. 2b, 34 variationally determined spectral moments for each of five q values are extended (Table III) to sufficient numbers of recurrence coefficients to obtain the fully convergent Tschebyscheff approximations for $1 \leqslant q \leqslant 4$ a.u shown in Fig. 3b. It is found that a fourfold extension is required to obtain complete convergence in this interval, corresponding formally to the use of approximately 170 power moments. The moment equations need not be solved, however, since the recurrence coefficients are available in closed form (Eqs. (22) and (23)). The resulting spectra (Fig. 3b) are evidently very smooth and in excellent accord with the correct curves for $1 \leqslant q \leqslant 4$ a.u. When additional extended recurrence coefficients are introduced, corresponding to an eightfold extension, the Tschebycheff result for the $q = 5$ a.u. spectrum is also convergent, within the accuracy of the coefficients of Table II. Use of ad hoc smoothing techniques on the cumulative distribution of Eq. (16a) in lower orders can also give convergent profiles, although it is satisfying that the Tschebycheff density can be made fully convergent employing the well-defined recurrence-coefficient extension procedure [24].

In addition to the results shown in Figs. 2 and 3, Stieltjes and Tschebyscheff profiles have been constructed employing various polynomial moments [28]. Approximately sixty Jacobi moments, calculated employing previously described recurrence techniques [21], are found to provide highly stable moment problems and convergent Stieltjes and Tschebyscheff approximations to the Bethe surface in atomic hydrogen when appropriately extended recurrence coefficients are used. Although the moment problem associated with the use of Jacobi moments is more stable than that associated with an equal number of power moments, the rate of convergence of the Stieltjes and Tschebyscheff approximations are found to be approximately the same in each case, with equal numbers of recurrence coefficients providing similarly reliable results.

In Table IV we show the complex poles of the 10th-order Tschebyscheff derivative (Eq. (16b)) obtained by employing the coefficients of Table II for $q = 1$ to 5. These poles are evidently distributed in accordance with the general shapes of the associated spectra. For $q = 1$, they lie along an approximate ray making a relatively small angle with the real axis, whereas, for the larger values of q, there are high-energy poles parallel to the real axis in the approximate vicinity of the Bethe ridge. Moreover, use of only the discrete portions of the spectral moments in atomic hydrogen results in Tschebyscheff densities (not shown) having poles very near the real axis in the appropriate discrete interval. Similarly, use of the continuum portions of the spectral moments results in densities (not shown) having poles that fall on rays beginning at

TABLE IV

Complex Poles of the Tschebyscheff Derivative $G^{(10)}(z, q)$ for the Bethe Surface in Atomic Hydrogen[a]

$q = 1$		$q = 2$		$q = 3$		$q = 4$		$q = 5$	
Real	Imaginary	Real	Imaginary	Real	Imaginary	Real	Imaginary	Real	Imaginary
0.37500	0.00049	0.37500	0.00083	0.37501	0.00101	0.37501	0.00110	0.37501	0.00114
0.44858	0.01304	0.45091	0.01692	0.45209	0.01871	0.45266	0.01955	0.45296	0.01998
0.51267	0.03974	0.52751	0.05006	0.53472	0.05520	0.53812	0.05764	0.53991	0.05891
0.61950	0.07650	0.66392	0.10134	0.68728	0.11618	0.69852	0.12354	0.70441	0.12745
0.79391	0.13277	0.90729	0.19053	0.97904	0.23847	1.01559	0.26534	1.03508	0.28017
1.07995	022956	1.34363	0.34232	1.58376	0.50642	1.72773	0.63441	1.80872	0.71649
1.58100	0.43277	2.07505	0.56424	2.85764	0.94922	3.63590	1.53033	4.25581	2.18831
2.63141	1.00994	3.22400	1.01041	4.72648	1.32534	7.02584	1.97169	10.10969	2.95394
5.76177	3.61697	5.80963	3.05523	7.31907	2.89572	10.19554	3.04809	14.27655	3.40918

[a] Values, in Hartree atomic units, obtained from a complex root search of Eq. (16b) with $n = 10$ for $q = 1$ to 5 a.u., constructed employing the polynomial recurrence coefficients of Table II.

the ionization threshold. In the latter case, the rate of convergence of the Tschebyscheff density with the number of moments employed is found to be similar to that obtained using the total spectral moments. These results indicate that spectral moments can be employed to characterize all or only a given portion of a corresponding generalized oscillator-strength distribution uniquely.

C. *Van Hove Correlation Functions*

The convergence of the Bethe surface with increasing numbers of spectral moments indicated in the preceding subsection assures corresponding convergence of the associate scattering cross sections, since the integrands are smooth slowly-varying functions of energy over the interval of the defining distribution, and the integrals are evaluated using an optimal set of generalized quadratures. By contrast, determination of the time autocorrelation functions of atomic systems from spectral moments and corresponding Gaussian quadratures is much more difficult, since the integrand in this case is a highly oscillatory function.

It is found in the present development that the moment-theory procedure in low orders gives quadrature approximations to correlation functions that are in good accord with the correct values over short time intervals, but which exhibit unphysical oscillations for longer times. Quadrature points and weights providing both upper and lower principal representations, corresponding to Radau quadratures having one point fixed at the lower and upper ends of the integration interval [8, 32], respectively, are employed in order to test the time range of mutual agreement for given numbers of moments [28]. It is found that the mutual agreement between upper and lower principal representation results (not shown) becomes poor for those times at which agreement with the correct values is also poor [28], providing an a priori method for assessing the reliability of moment approximations to time correlation functions.

Although quadrature approximations to time autocorrelation functions can lead to unphysical long-time oscillations when small numbers of moments are employed, use of sufficient numbers of spectral moments insures that these effects are minimized. In Fig. 4, we show the real parts of time autocorrelation functions for atomic hydrogen obtained from the quadrature expression

$$\Phi(q, t) = (q^2/2) \sum_{i=1}^{n} (f_i(q, n)/\varepsilon_i(q, n))\, e^{i\varepsilon_i(q,n)t} \tag{24}$$

employing variationally determined moments and the recurrence coefficient extension procedure (Eqs. (22) and (23), Tables II and III). Large numbers of moments (374), corresponding to a tenfold extension, are required to provide the results of Fig. 4, which are in excellent agreement with the correct values for $q = 0$ to 4 a.u. For $q = 5$ a.u., however, there is a discernible difference between the correct and moment-theory results for $t \gtrsim 0.5$ a.u. This is a consequence of inaccuracies in the polynomial recurrence coefficients of Table II for $q = 5$, which, as indicated above, are accurate

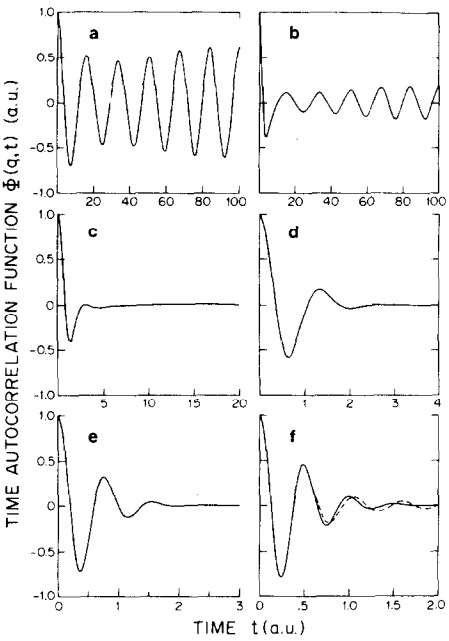

FIG. 4. Real parts of time autocorrelation functions in atomic hydrogen normalized to $t = 0$ values: (—) correct values [4]; (---) values obtained from Eq. (24) employing variationally determined recurrence coefficients (Table II) and the extension procedure of Eqs. (22) and (23). Values for q: (a) 0; (b) 1; (c) 2; (d) 3; (e) 4; (f) 5. All values in Hartree atomic units.

to only two or three significant figures. Consequently, introduction of additional recurrence coefficients using the extension procedure in this case does not lead to agreement between the correct and moment-theory results for the autocorrelation function. The results of Fig. 4 indicate that use of modest numbers of accurate spectral moments and the extension approach of Eqs. (22) and (23) can provide convergent Van Hove time autocorrelation functions for atomic targets.

It is also possible to construct separately the discrete and continuum portions of the Van Hove functions by employing the appropriate moments and quadratures. In order to accomplish this evaluation, it is necessary to partition variationally calculated pseudospectra into discrete and continuum contributions, as in the evaluation of the corresponding portions of the Bethe surface indicated above. Alternatively, formulation of procedures for direct determinations of autocorrelation functions without reference to corresponding spectra or pseudospectra would be highly desirable [3], a topic beyond the scope of the present study.

D. *Principal Pseudostates*

In accordance with previous observations [33], it is anticipated that the pseudostates of Eqs. (9) for an arbitrary basis will generally provide L^2 approximations to the associated correct scattering functions at energies above the

ionization threshold. The correct scattering normalization is generally not obtained from L^2 variational calculations, however, and additional considerations must be employed to determine the complete scattering function [33]. Principal pseudostates obtained from the L^2 moment-theory development provide a general method for determining the correct normalization factors [14–16]. In the case of atomic hydrogen, the development is particularly straightforward, since the Laguerre functions of order $n + l + 1/2l + 2$ employed in the variational development provide a basis appropriate for determining principal pseudostates directly from the variational development [28]. As indicated above, N of the Laguerre functions of order $n + l + 1/2l + 2$ provide a pseudospectrum $(\varepsilon_i^{(l)}, \Phi_i^{(l)}; i = 1, N)$ from Eqs. (9) that gives directly Nth-order Gaussian quadratures in the forms

$$\varepsilon_i^{(l)} = \langle \Phi_i^{(l)} | H_0 - E_0 | \Phi_i^{(l)} \rangle, \tag{25a}$$

$$f_i^{(l)} = 2\varepsilon_i^{(l)} |\langle \Phi_i^{(l)} | r^l P_l(\cos\theta) | \phi_0 \rangle|^2, \qquad i = 1, 2, \ldots, N, \tag{25b}$$

corresponding to the spectrum of Eqs. (21). Because the first $2N$ power moments of the spectrum are reproduced correctly by the quadratures of Eqs. (25), the corresponding pseudospectrum of transition energies and eigenfunctions is designated

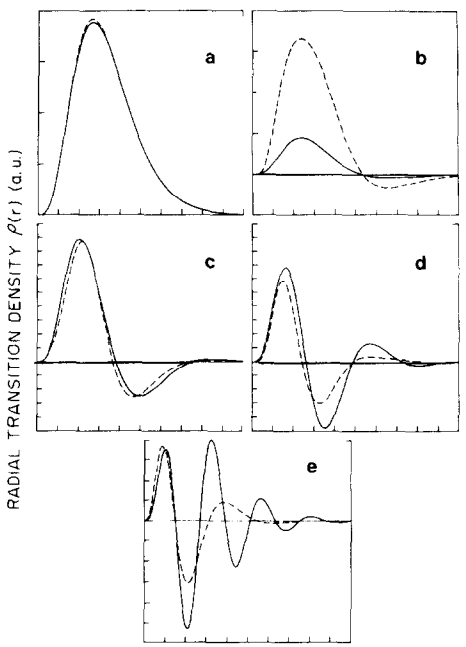

FIG. 5. Dipole ($l = 1$) radial transition densities in atomic hydrogen over the interval $0 \leqslant r \leqslant 10$ a.u.; (—) correct results of Eq. (30) for (a) $E_1 = -0.1247$; (b) $E_2 = -0.0215$; (c) $E_3 = 0.1834$; (d) $E_4 = 0.7559$; (e) $E_5 = 3.2068$ [36]; (---) 5th-order principal pseudostate results of Eq. (29). The ordinate scales employ tick mark intervals of 0.1 a.u. in each case. All values in Hartree atomic units.

a principal representation of the spectrum, in accordance with generally accepted moment-theory usage [8].

To clarify the nature of pseudostate approximations to scattering functions, it is convenient to compare the l-wave multipole oscillator strengths obtained from a principal pseudospectrum ($\Phi_i^{(l)}$, $\varepsilon_i^{(l)}$; $i = 1, n$) in l-wave symmetry with the corresponding correct values of Eqs. (21). The former can be written in the form

$$f_i^{(l)} = 2\varepsilon_i^{(l)} |\langle \Phi_i^{(l)} | r^l P_l(\cos\theta) | \phi_0 \rangle|^2$$
$$= 2\varepsilon_i^{(l)} \left[\int_0^\infty R_i^{(l)}(r)\, R_{1s}(r)\, r^{l+2}\, dr \int_0^{2\pi} \int_0^{\pi} Y_l^0(\theta)\, P_l(\cos\theta)\, Y_0^0\, d\Omega \right]^2, \quad (26a)$$

with $R_i^{(l)}(r)$ the radial portion of $\Phi_i^{(l)}$, whereas the continuum density of Eq. (21c) is

$$g^{(l)}(\varepsilon) = 2\varepsilon |\langle \phi_\varepsilon^{(l)} | r^l P_l(\cos\theta) | \phi_0 \rangle|^2,$$
$$= 2\varepsilon \left[\int_0^\infty R_\varepsilon^{(l)}(r)\, R_{1s}(r)\, r^{l+2} \int_0^{2\pi} \int_0^{\pi} Y_l^0(\theta)\, P_l(\cos\theta)\, Y_0^0\, d\Omega \right]^2, \quad (26b)$$

with $R_\varepsilon^{(l)}(r)$ the l-wave multipole Coulomb function [34, 35]. Since the principal pseudostate $\Phi_i^{(l)}$ is unity normalized, while $\phi_\varepsilon^{(l)}(r)$ is delta-function normalized in the

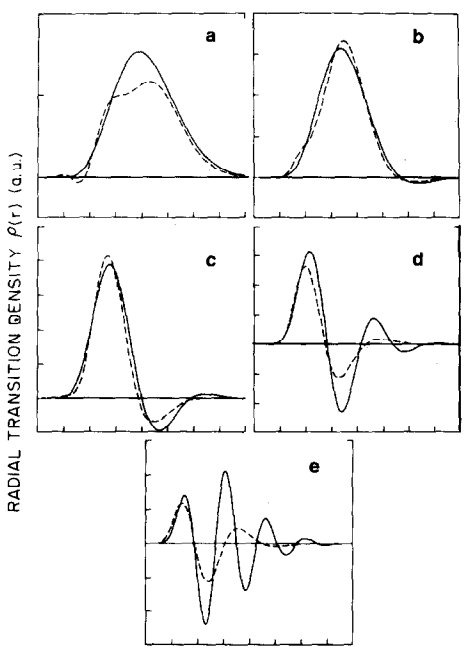

FIG. 6. As in Fig. 5 for hexadecapole ($l = 4$) densities over the interval $0 \leqslant r \leqslant 16$ a.u. (a) $E_1 = 0.0180$; (b) $E_2 = 0.1269$; (c) $E_3 = 0.3395$; (d) $E_4 = 0.7197$; (e) $E_5 = 2.0421$. The ordinate scales employ tick marks of 10.0 a.u. in each case.

energy, the oscillator strength of Eq. (26a) is generally not equal to the density of Eq. (26b) evaluated at $\varepsilon = \varepsilon_i^{(l)}$. The former strength (Eq. (26a)), however, can be made equal to the latter density (Eq. (26b)) if the pseudostate $\Phi_i^{(l)}$ is renormalized in the form

$$\Phi_i^{(l)} \to N_i^{(l)} \Phi_i^{(l)}, \tag{27}$$

where the normalization factor $N_i^{(l)}$ is given by

$$N_i^{(l)} = [\, g^{(l)}(\varepsilon_i^{(l)})/f_i^{(l)}]^{1/2}, \tag{28}$$

and the correct density $g^{(l)}(\varepsilon_i^{(l)})$ is approximated by the Stieltjes–Tschebyscheff development. The latter may be constructed directly from the variationally determined pseudospectrum, since the latter provides a principal representation of the correct multipole oscillator-strength distribution. Consequently, correctly normalized L^2 approximations $N_i^{(l)}\Phi_i^{(l)}$ to the scattering functions $\phi_\varepsilon^{(l)}$ are obtained directly from the variational development when principal pseudostates are employed. To test the reliability and convergence of the development, the radial densities

$$\tilde{\rho}^{(l)}(r) = N_i^{(l)} R_i^{(l)}(r)\, R_{1s}(r)\, r^{l+2} \tag{29}$$

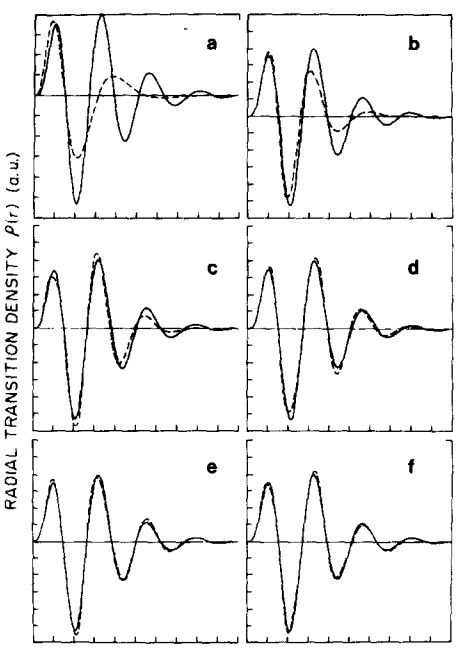

FIG. 7. Dipole ($l = 1$) radial transition densities in atomic hydrogen over the interval $0 \leqslant r \leqslant 10$ a.u.; (—) correct results of Eq. (30) for (a) $E_5^{(5)} = 3.2068$; (b) $E_{12}^{(14)} = 3.2507$; (c) $E_{19}^{(23)} = 3.3551$; (d) $E_{25}^{(31)} = 3.1949$; (e) $E_{32}^{(40)} = 3.2902$; (f) $E_{38}^{(48)} = 3.2078$; (---) principal pseudostate results of indicated orders obtained from Eq. (29). The ordinate scales employ tick marks of 0.1 a.u. in each case. All values in Hartree atomic units.

obtained from Eqs. (25)–(28) are compared with the corresponding correct densities

$$\rho^{(l)}(r) = R_{\varepsilon}^{(l)}(r)\, R_{1s}(r)\, r^{l+2}, \qquad \varepsilon = \varepsilon_i^{(l)}, \tag{30}$$

for a considerable range of values of l and a great many principal pseudospectra in atomic hydrogen [28].

In Figs. 5 and 6, we show as examples the densities of Eq. (29) for $l = 1$ and 4, respectively, obained from 5th-order principal pseudospectra, in comparison with the correct corresponding results of Eq. (30) [36]. Although only five principal pseudostates are used in each case, it is seen that the spectra are uniformly spanned and that the L^2 results are in generally good agreement with the correct values. Because the second principal pseudostate in the $l = 1$ case is higher lying than the correct $3p$ state, the corresponding radial densities are in poor accord in this case. This is to be expected, since the second principal pseudostate represents also the higher-lying discrete $1s \rightarrow np$ transitions, which contribute nonnegligibly to the spectrum. By contrast, in the $l = 4$ case, only the continuous portion contributes substantially to the correct spectrum, and, consequently, the 5th-order principal pseudostates all fall above threshold. It is seen that the highest-lying result in each case is in poorest agreement with the corresponding correct values. Clearly,

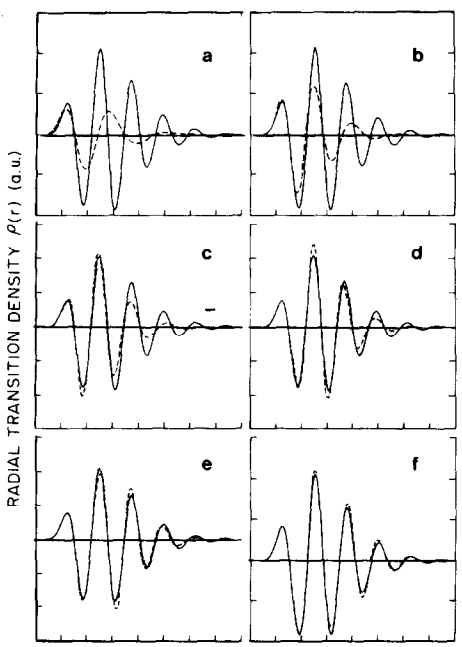

FIG. 8. As in Fig. 7 for hexadecapole ($l = 4$) densities over the interval $0 \leqslant r \leqslant 16$ a.u. (a) $E_7^{(7)} = 3.2688$; (b) $E_{14}^{(16)} = 3.1497$; (c) $E_{21}^{(25)} = 3.2301$; (d) $E_{28}^{(34)} = 3.3022$; (e) $E_{34}^{(42)} = 3.2019$; (f) $E_{40}^{(50)} = 3.1389$. The ordinate scales employ tick marks of 10.0 a.u. in each case.

additional functions, corresponding to higher-order principal pseudospectra, are required to achieve convergence to the higher-lying continuum states.

In Figs. 7 and 8, we show the results of Eq. (29) as functions of increasing order for $l = 1$ and 4, respectively, obtained at energies corresponding approximately to the position of the highest-lying principal pseudostate of Fig. 5. It is seen that as the order of the principal pseudospectrum, or the number of basis functions employed, is increased, the corresponding radial densities converge smoothly to the correct results. Similarly good convergence is also obtained at lower energies and other l values. At higher energies, additional numbers of functions are required to achieve convergence, since the correct scattering functions and transition densities become highly oscillatory. It is important to note in this connection that principal pseudostates of any order are always distributed over the important or spectrally dense portions of

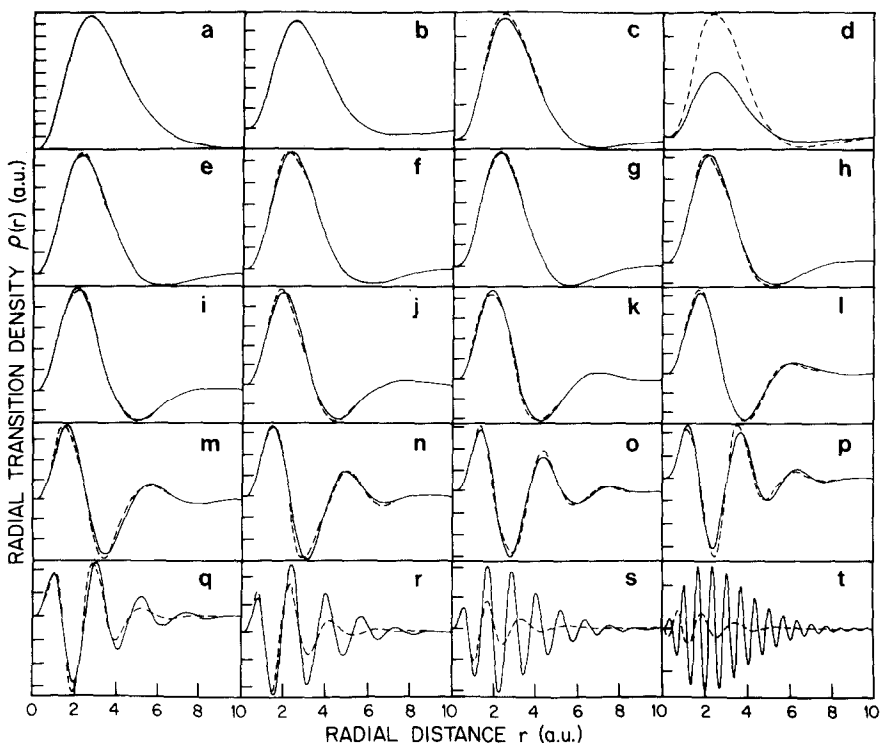

FIG. 9. Dipole ($l = 1$) radial transition densities in atomic hydrogen over the interval $0 \leqslant r \leqslant 10$ a.u.; (—) correct results of Eq. (30) for (a) $\tilde{E}_1 = -0.1250$; (b) $\tilde{E}_2 = -0.0556$; (c) $\tilde{E}_3 = -0.0311$; (d) $\tilde{E}_4 = -0.0154$; (e) $\tilde{E}_5 = 0.00621$; (f) $\tilde{E}_6 = 0.0367$; (g) $\tilde{E}_7 = 0.0776$; (h) $\tilde{E}_8 = 0.1312$; (i) $\tilde{E}_9 = 0.2011$; (j) $\tilde{E}_{10} = 0.2930$; (k) $\tilde{E}_{11} = 0.4153$; (l) $\tilde{E}_{12} = 0.5811$; (m) $\tilde{E}_{13} = 0.8122$; (n) $\tilde{E}_{14} = 1.146$; (o) $\tilde{E}_{15} = 1.652$; (p) $\tilde{E}_{16} = 2.468$; (q) $\tilde{E}_{17} = 3.908$; (r) $\tilde{E}_{18} = 6.815$; (s) $\tilde{E}_{19} = 14.15$; (t) $\tilde{E}_{20} = 43.54$. (---) 20th-order principal pseudostate results of Eq. (29). Ordinate scale intervals correspond to 0.01 a.u. for the first four figures, 0.05 a.u. for the remaining figures. All values in Hartree atomic units.

the corresponding spectrum as a consequence of satisfying the appropriate moment equations.

In Fig. 9, we show the results of Eqs. (29) and (30) for $l = 1$ obtained from a 20th-order principal pseudospectrum. Evidently, 12 of the 20 states obtained fall within $\sim$15 eV of threshold, in which region the major portion of the dipole ($l = 1$) oscillator strength is found. Moreover, even the higher-lying results are in good agreement with the correct values, although the highly oscillatory behaviors of the last few densities are not satisfactorily reproduced. At these very high energies, however, the corresponding Coulomb functions are well represented by their simple analytic asymptotic forms, and detailed computations are somewhat irrelevant in any event [34, 35].

V. Concluding Remarks

Theoretical studies of high-energy inelastic electron scattering cross sections and related quantities generally entail construction, in some approximation, of the discrete and continuum excited eigenstates of the target atom or molecule. The procedures described here provide a means for avoiding the customary eigenstates, but nevertheless give all the information obtained from the conventional approaches. Square-integrable basis functions and partial-wave expansions are seen to be sufficient for determinations of appropriate spectral moments and related polynomial recurrence coefficients. Convergent approximations to the associated Bethe surface are obtained from these and the Stieltjes–Tschebyscheff technique when the important extension procedure is used in the construction of a complete set of polynomial recurrence coefficients for atomic hydrogen. These results suggest that a similar approach, in which finite L^2 basis-set calculations are supplemented with appropriate asymptotic information, can be employed in moment-theory investigations of the Bethe surfaces of more complex atomic and molecular targets.

The Van Hove time autocorrelation functions in atomic hydrogen are seen to involve oscillating integrands and spectral distributions that extend to high energy. Consequently, quadrature determinations are expected to be slowly convergent. Nevertheless, it is seen that the Stieltjes–Tschebyscheff technique provides fully convergent values when the previously described polynomial recurrence coefficient extension procedure is employed. As an alternative to the development reported here, in which the correlation functions are determined from moments of the known spectral distribution, it is of considerable interest to investigate direct determinations of Van Hove correlation functions employing semiclassical and related approximations and subsequent Fourier inversion to determine corresponding spectral distributions.

In further clarification of the moment-theory approach to inelastic scattering cross sections, and of the basis of its reliability, comparisons are made of the correct and L^2 approximations to scattering functions associated with the continuous spectrum in atomic hydrogen. It is seen that previously defined principal pseudostates provide

excellent approximations, including the correct normalization, to radial transition densities derived from the regular Coulomb waves evaluated at corresponding energies. This suggests that the ultimate basis for the reliability of the moment-theory approach to high-energy inelastic scattering cross sections is to be found in L^2 variational calculations of the appropriate excitation/ionization spectra. Because the approach can employ the conventional technology of L^2 basis-set calculations, it is anticipated that the Stieltjes–Tschebyscheff technique will be particularly useful for studies of the Bethe surfaces and related cross sections of molecular targets [37].

ACKNOWLEDGMENTS

Acknowledgment is made to donors of the Petroleum Research Fund, administered by the American Chemical Society, and to the National Science Foundation for partial support of this work. It is a pleasure to thank W. P. Reinhardt and the JILA Fellows, and S. R. Langhoff, R. Jaffee, and J. O. Arnold, NASA Ames Research Center, for their kind hospitality to and support of P. W. L., to thank W. J. Meath for his kind hospitality to D. J. M., to acknowledge the computational assistance of C. T. Corcoran and S. L. Seidman, and to thank R. A. Bonham for helpful comments.

REFERENCES

1. H. A. BETHE, *Ann. Phys.* **5** (1930), 325.
2. M. INOKUTI, *Rev. Mod. Phys.* **43** (1971), 297; M. INOKUTI, Y. ITIKAWA, AND J. E. TURNER, **50**(1978), 23.
3. R. A. BONHAM, *in* "Electron Spectroscopy," Vol. III (C. R. Brundle and A. D. Baker, Eds.), Academic Press, New York, 1979.
4. D. J. MARGOLIASH AND P. W. LANGHOFF, *J. Comput. Phys.* **49** (1983), 44.
5. P. W. LANGHOFF, *in* "Electron-Molecule and Photon-Molecule Collisions" (T. N. Rescigno, B. V. McKoy, and B. Schneider, Eds.), pp. 183–224, Plenum, New York, 1979.
6. P. W. LANGHOFF, *in* "Theory and Applications of Moment Methods in Many-Fermion Systems" (B. J. Dalton, S. M. Grimes, J. P. Vary, and S. A. Williams, Eds.), p. 191–212, Plenum, New York, 1980.
7. P. W. LANGHOFF, N. PADIAL, G. CSANAK, T. N. RESCIGNO, AND B. V. MCKOY, *Int. J. Quantum Chem.* **S14** (1980), 285.
8. J. A. SHOHAT AND J. D. TAMARKIN, "The Problem of Moments," Mathematical Surveys **1** American Mathematical Society, Providence, 1950.
9. C. T. CORCORAN AND P. W. LANGHOFF, *J. Math. Phys.* **18** (1977), 651.
10. U. W. HOCHSTRASSER, *in* "Handbook of Mathematical Functions" (M. Abramowitz and I. A. Stegun, Eds.), Chap. 22, Dover, New York, 1965.
11. P. W. LANGHOFF, *J. Chem. Phys.* **57**(1972), 2604.
12. P. W. LANGHOFF, *Int. J. Quantum Chem.* **S8** (1974), 347.
13. P. W. LANGHOFF AND S. L. SEIDMAN, *Chem. Phys. Lett.* **27** (1974), 195.
14. P. W. LANGHOFF, *Chem. Phys. Lett.* **22** (1973), 60.
15. P. W. LANGHOFF AND C. T. CORCORAN, *J. Chem. Phys.* **61** (1974), 146.
16. P. W. LANGHOFF, J. S. SIMS, AND C. T. CORCORAN, *Phys. Rev. A* **10** (1974), 829.
17. J. O. HIRSCHFELDER, W. BROWN, AND S. T. EPSTEIN, *Adv. Quantum Chem.* **1** (1964), 255; R. JACKIW, *Phys. Rev.* **157** (1967), 1220.
18. P. W. LANGHOFF AND M. KARPLUS, *J. Chem. Phys.* **52** (1970), 1435.

19. S. T. EPSTEIN, "The Variation Method in Quantum Chemistry," Academic Press, New York, 1974.
20. C. T. CORCORAN AND P. W. LANGHOFF, *Chem. Phys. Lett.* **41** (1976), 609.
21. R. A. SACK AND A. F. DONOVAN, *Numer. Math.* **18** (1972), 465.
22. C. T. CORCORAN, Ph. D. Dissertation, Indiana University, 1977, unpublished.
23. P. W. LANGHOFF AND C. T. CORCORAN, *Chem. Phys. Lett.* **40** (1976), 367.
24. P. W. LANGHOFF, C. T. CORCORAN. J. S. SIMS, F. WEINHOLD, AND R. M. GLOVER, *Phys. Rev. A* **14** (1976), 1042.
25. P. W. LANGHOFF, C. T. CORCORAN, AND J. S. SIMS *Phys. Rev. A* **16** (1977), 1513.
26. C. K. AU, *J. Phys. B* **11** (1978), 2781; **13** (1980), 1023.
27. E. A. HYLLERAAS, *Z. Phys.* **48** (1928), 469; H. SHULL AND P.-O. LOWDIN, *J. Chem. Phys.* **23** (1955), 1362; **30** (1959), 617.
28. D. J. MARGOLIASH, Ph. D. Dissertation, Indiana University, 1980, unpublished.
29. M. R. FLANNERY, *Phys. Rev.* **183** (1969), 231; M. R. FLANNERY AND H. LEVY, *J. Phys. B* **2** (1969), 324. A power-series expansion employed by these authors has been avoided in the present development through the use of generating-function techniques, resulting in more compact final integral expressions than those reported. See [28] for additional details.
30. H. F. WELLENSTEIN, R. A. BONHAM, AND R. C. ULSH, *Phys. Rev. A* **8** (1973), 304.
31. W. GAUTSCHI, *Math. Comput.* **22** (1968), 251.
32. P. W. LANGHOFF, *Chem. Phys. Lett.* **9** (1974), 89.
33. A. U. HAZI AND H. S. TAYLOR, *Phys. Rev. A* **1**, (1970), 1109.
34. H. A. BETHE AND E. E. SALPETER, "Quantum Mechanics of One- and Two-Electron Atoms," Academic Press, New York, 1957.
35. G. ARFKEN, "Mathematical Methods for Physicists," Chap. 13, Academic Press, New York, 1970. See also Chaps. 13 and 14 in [10].
36. In the case of discrete transitions, the renormalization of Eqs. (27) and (28) is not required, and the corresponding correct radial densities are evaluated using the appropriate hydrogenic eigenfunctions [33].
37. Refined procedures for construction of L^2 moment-theory approximations to atomic and molecular Schrödinger spectra are described by P. W. Langhoff in "Proceedings of the NATO Advanced Study Institute on Methods in Computational Molecular Physics" (G. H. F. Diercksen and S. Wilson, Eds.), Reidel, Dordrecht, 1982.